Auxeticity in biosystems: an exemplification of its effects on the mechanobiology of heterogeneous living cells

Sundeep Singh & Roderick Melnik

Published online: 16 Aug 2021.

Submit your article to this journal

Article views: 82

View related articles

View Crossmark data

Taylor & Francis
Taylor & Francis Group

Check for updates

Auxeticity in biosystems: an exemplification of its effects on the mechanobiology of heterogeneous living cells

Sundeep Singh[a] (ID) and Roderick Melnik[a,b] (ID)

[a]MS2Discovery Interdisciplinary Research Institute, Wilfrid Laurier University, Waterloo, Ontario, Canada; [b]BCAM – Basque Center for Applied Mathematics, Bilbao, Spain

ABSTRACT

Auxeticity (negative Poisson's ratio) is the unique mechanical property found in an extensive variety of materials, such as metals, graphene, composites, polymers, foams, fibers, ceramics, zeolites, silicates and biological tissues. The enhanced mechanical features of the auxetic materials have motivated scientists to design, engineer and manufacture man-made auxetic materials to fully leverage their capabilities in different fields of research applications, including aeronautics, medical, protective equipments, smart sensors, filter cleaning, and so on. Atomic force microscopy (AFM) indentation is one of the most widely used methods for characterizing the mechanical properties and response of the living cells. In this contribution, we highlight main consequences of auxeticity for biosystems and provide a representative example to quantify the effect of nucleus auxeticity on the force response of the embryonic stem cells. A parametric study has been conducted on a heterogeneous stem cell to evaluate the effect of nucleus diameter, nucleus elasticity, indenter's shape and location on the force-indentation curve. The developed model has also been validated with the recently reported experimental studies available in the literature. Our results suggest that the nucleus auxeticity plays a profound role in cell mechanics especially for large size nucleus. We also report the mechanical stresses induced within the hyperelastic cell model under different loading conditions that would be quite useful in decoding the interrelations between mechanical stimuli and cellular behavior of auxetic biosystems. Finally, current and potential areas of applications of our findings for regenerative therapies, tissue engineering, 3D/4D bioprinting, and the development of meta-biomaterials are discussed.

1. Introduction

In nature, auxetic (or negative Poisson's ratio) behavior has been found in a wide variety of materials including nanomaterials (e.g. graphene, black phosphorous, carbon nanotubes), foam, silicates, zeolites, and biological materials (e.g. human tendons, nuclei in embryonic stem cells, arteries, skin) (Gatt et al. 2015; Wang et al. 2015; Li et al. 2019). Unlike conventional materials, auxetic materials become thinner when compressed and thicker when stretched (HM Kolken and Zadpoor 2017; Krishnaswamy et al. 2020; Mardling et al. 2020). Auxeticity provides several unique benefits compared to conventional materials, like higher shear resistance, fracture toughness, indentation resistance, energy dissipation and acoustic absorption capabilities, as well as variable permeability and natural ability to form dome-shaped surfaces (synclastic behavior). These unusual and even unprecedented mechanical properties of auxetic materials

have motivated scientists to design, engineer and manufacture man-made such materials (often known as 'auxetic metamaterials') that have shown enormous potential in the fields of aerospace, biomedicine, protective equipment, packing, soft robotics, intelligent sensors, actuators, acoustic cloaking and new functional structures (Cabras and Brun 2014; Gatt et al. 2015; Warner et al. 2017; Ren et al. 2018; Domaschke et al. 2019; Li et al. 2019; Soyarslan et al. 2019; Wang Z et al. 2020; Krishnaswamy et al. 2021). This field of auxetic metamaterials has also gained a rapid boost during the last few years due to the recent advances in design and manufacturing technology, such as additive manufacturing (3D printing) techniques, that allows to fabricate geometrical designs of arbitrary complex structures at the macro-, micro-, and nano-scales (Wang et al. 2015; HM Kolken and Zadpoor 2017; Warner et al. 2017; Zadpoor 2019; Wang Z et al. 2020; Zadpoor 2019). Auxetic meta-biomaterials

have already received a lot of attention in the designing and improving the longevity of orthopedic implants and holds great promise as a future group of biomaterials in designing a range of biomedical devices for different applications. At the same time, there are still multiple manufacturing-related and/or design-related challenges that need to be overcome for expanding the horizon of research into these meta-biomaterials (Zadpoor 2020).

Biological cells are constantly exposed and must respond to a variety of extracellular and intracellular mechanical loads *in vivo* (Haase and Pelling 2015). This continual process of sensing, transmission and responding to the external mechanical stimuli is known as mechanotransduction. It is critical for maintenance of normal cell functioning and development, such as in growth, motility, differentiation, proliferation and apoptosis, and the application of this process has attracted widespread attention in modern medical therapies such as in the fields of tissue engineering, regenerative medicine and some disease treatments (Haase and Pelling 2015; Basoli et al. 2018; Liu et al. 2019; Singh et al. 2020). In recent years, tremendous focus has been given to understanding how the mechanical properties influence the cellular dynamics with respect to its surrounding microenvironment. A better understanding of mechanotransduction mechanisms would pave the way for further improvements and inventions in the areas of early disease diagnoses and treatments, as well as drug development. Furthermore, advances in the mechanics of biological cells have fueled the development of several biophysical techniques to measure the mechanical properties of the cell, viz., optical stretcher, atomic force microscopy (AFM), magnetic tweezer, micropipette aspiration and traction force microscopy (Addae-Mensah and Wikswo 2008; Ding et al. 2017; Basoli et al. 2018). Among these experimental techniques, AFM has become the most popular and powerful tool for mechanical characterization of both healthy and diseased cells at different stages of the cell-cycle, due to its enhanced capabilities in precise force and location control (Melnik et al. 2009; Basoli et al. 2018; Krieg et al. 2019; Liu et al. 2019; Garcia et al. 2020). The experimental sample preparation of the AFM requires the deposition, absorption or culture of the cell specimen on the rigid support (e.g. mica, glass or silicon) (Garcia and Garcia 2018b). Once prepared, the sample is indented with a tip-cantilever system and the force-distance (or indentation) curve is recorded at the AFM tip that reflects the deformation of the cantilever against a prescribed force into the sample, which is utilized to quantify the mechanical properties of cells (Basoli et al. 2018).

Several numerical studies of indentation tests have been reported in the literature for the mechanical characterization of biological entities at the cellular and subcellular scales (Barreto et al. 2013; Bonilla et al. 2015; Digiuni et al. 2015; Ding et al. 2017; Garcia and Garcia 2018b, 2018a; Dagro A et al. 2019; AM Dagro and Ramesh 2019). A contact mechanics model is routinely applied to capture the cell mechanics utilizing: Hertz, Sneddon, Johnson–Kendall–Roberts (JKR), Tatara, Multiscale Decomposition Analysis, and the Multi-Regime models (Hertz 1882; Sneddon 1965; Tatara 1989; Basoli et al. 2018). However, the most common drawback of these methods is the use of rough approximation of the real conditions, which includes the assumption of treating the biological sample, AFM tip, and substrate as homogenous bodies with well-defined idealized geometries, which is far from reality and is thus highly prone to errors (Basoli et al. 2018; Liu et al. 2019). To address this issue, the application of finite element method (FEM) is quite promising for modeling AFM nanoindentations to more accurately capture the nuances of the force transduction process within the living cells (Fallqvist et al. 2016; Efremov et al. 2017; Kasas et al. 2017; Liu et al. 2019; Saeed and Weihs 2019; Tang et al. 2019; Wang L et al. 2020). Notably, the surface effect on the mechanical response of cells under forces have been examined by FEM in Ding et al. (2017; 2018). Furthermore, it is noteworthy to mention that the experimental studies have confirmed that when the embryonic stem cells differentiate and are in the transition period leaving the state of pluripotency, their nucleus becomes auxetic, i.e. possess a negative Poisson's ratio (Pagliara et al. 2014; Hodgson et al. 2017; Tripathi and Menon 2019). This is a highly unique property of self-renewing stem cells as compared to the nuclei of other biological cells. To the best of the authors' knowledge, there has been no numerical study reported in the literature accounting for the auxeticity of stem cells during AFM indentation. Such a study would provide an important representative example of auxeticity in biosystems in general and in living cells in particular.

In what follows, we report FEM based numerical model to quantify the effect of nucleus auxeticity on the cell deformation during AFM indentation under various mechanical stimuli. A comparative analysis has been conducted to evaluate the impact of nucleus auxeticity on the force indentation response during AFM. Parametric studies have also been carried out to investigate the role of nucleus diameter, indenter
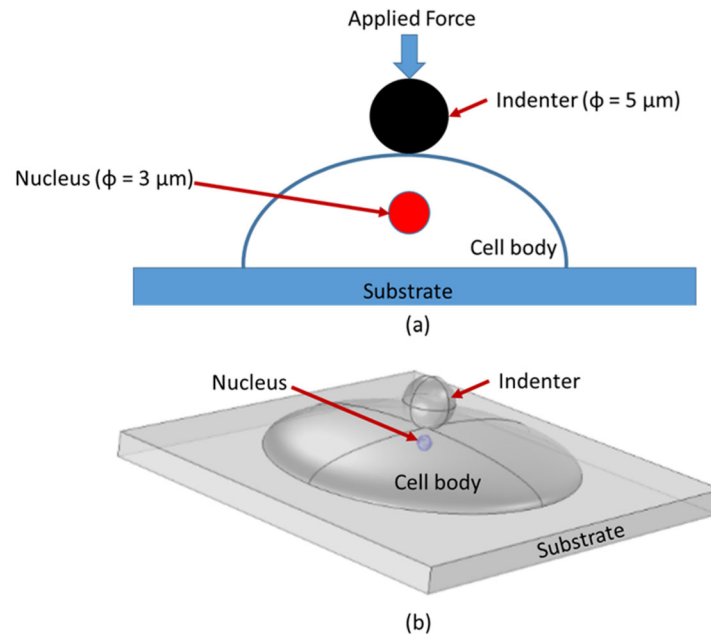
Figure 1. (a) Schematic of the simplified model of AFM indentation of adherent stem cell with a spherical indenter. (b) 3 D CAD model of AFM indentation considered in the present numerical study.

shape, and location on the stress distribution within the auxetic embryonic stem cells. The developed model will assist in our better understanding of the mechanotransduction process in the stem cell that could be quite useful in new discoveries in the field of regenerative medicine, as well as in other applications mentioned above.

2. Materials and methods

In this section, while focusing on the auxeticity in the living materials, we present the AFM indentation of embryonic stem cells as a good illustrative example of auxetic properties in biosystems. We will present the computational model of the single biological cell with the auxetic nucleus subjected to AFM indentation. The details about the mathematical framework, initial and boundary conditions, and material properties are also presented here.

2.1. Geometrical details of the model

The computational domain of the heterogeneous biological cell model considered in the present study is presented in Figure 1. Notably, the biological cell model in its simplified setting comprises of two distinct domains, viz., the cytoplasm and the nucleus, and the other components can be viewed as incorporated in the model as effective stiffness parameters (Fallqvist et al. 2016; Singh et al. 2020). Distinct material properties are provided for each layer of the

biological cell. The geometry of the adherent cell model is semi-ellipsoidal with a height and radius of $6\,\mu m$ and $15\,\mu m$, respectively, that has been motivated by Tang et al. (2019). Moreover, it should be noted that the nuclear shape and size for a given cell are significantly dependent on the cell type and cell morphology. For instance, the nucleus of most mammalian cells has a single spherically or ovoid shape with a diameter ranging from 5 to $20\,\mu m$ (Lammerding 2011). Also, cardiac myocytes and skeletal muscle cells are often multi-nucleated, while mature red blood cells do not contain a nucleus at all (Lammerding 2011). In the present study, the nucleus is located at the center of the cellular domain. It has been modeled as a sphere with a diameter varying from 3 to $5\,\mu m$. Notably, the considered nucleus diameter has been taken from the morphology of the living MDA-MB-231 cells and AFM has been performed utilizing the spherical indenter with $5\,\mu m$ diameter (Tang et al. 2019). Moreover, the biological cell (both matrix and nucleus) has been modeled as an incompressible hyperelastic material and the AFM indenter has been modeled as an isotropic elastic body with Young's modulus of 160 GPa and Poisson's ratio of 0.22. The Young's moduli of the cell-matrix and cell nucleus have been considered to be 0.25 kPa and 1 kPa respectively, while the Poisson's ratios of cell-matrix and cell nucleus have been considered to be 0.49 and 0.3, respectively (Katti and Katti 2017; Tang et al. 2019). Further, the auxetic nucleus has been modeled by considering the Poisson's ratio of

the cell nucleus as -0.3 (Pagliara et al. 2014; Tripathi and Menon 2019).

2.2. Governing equations

The equilibrium equation for the non-rigid mechanics is given by:

$$\rho \frac{\partial^2 u}{\partial t^2} = \sigma_{ij,j} + \overline{F}, \qquad (1)$$

where ρ is the density of the material, σ is the stress tensor $(i,j = 1,2,3$ are the tensor indices representing geometry's coordinate axes), u is the mechanical displacement vector, t is the time and $\overline{F}$ is the external body force. The stress-strain relationship for the linearly isotropic homogeneous elastic material is given by:

$$\sigma_{ij} = 2\mu\varepsilon_{ij} + \lambda\varepsilon_{kk}\delta_{ij}, \qquad (2)$$

where $\varepsilon_{ij} = \frac{1}{2}(u_{i,j} + u_{j,i})$ are the strain tensors, the terms λ and μ are the Lame's constants given by $\mu = \frac{E}{2(1+\nu)}$ and $\lambda = \frac{E\nu}{(1+\nu)(1-2\nu)}$, E is Young's modulus of elasticity, ν is the Poisson's ratio, and δ is the Kronecker delta function given by:

$$\delta_{ij} = \begin{Bmatrix} 1 \text{ for } i = j \\ 0 \text{ for } i \neq j \end{Bmatrix}. \qquad (3)$$

Further, in the present study, the biological cell has been modeled as incompressible hyperelastic material for which the stress-strain relationship is derived from the strain energy function. The Cauchy-stress tensor for the hyperelastic material can be expressed as (Holzapfel et al. 2000; Singh and Melnik 2020a):

$$\sigma = J^{-1} \frac{\partial W(F)}{\partial F} F^T, \qquad (4)$$

where F is the deformation gradient, J is the volume ratio $(= \det(F))$ and W is the strain energy. The neo-Hookean and Mooney-Rivlin models are widely used for capturing the indentation response of hyperelastic biological cells (Tang et al. 2019). The strain energy function of the hyperelastic biological cell considering the two-parameter Mooney-Rivlin model can be expressed as (Tang et al. 2019):

$$W = C_{10}(I_1 - 3) + C_{01}(I_2 - 3), \qquad (5)$$

where, as before, W is the strain energy, I_1 and I_2 are the first and second strain invariants, respectively, and C_{10} and C_{01} are the hyperelastic parameters. In the present study, we have used the neo-Hookean model (which is a special case of the Mooney-Rivlin model by setting $C_{01} = 0$) for modeling the force-indentation response during AFM of a biological cell. Further, for incompressible material (i.e. $\nu = 0.5$) $C_{10} = E/6$ (for small strain regime), where, as before, ν is the Poisson's ratio and E is Young's modulus. The model has also been extended to capture the viscoelastic nature of cytoplasm by adding two generalized Maxwell branches (with energy factor of 10 and relaxation times of 0.5 s and 50 s for the first and second branch, respectively) in the strain-energy density function given by Eq. 5 (Fallqvist et al. 2016).

2.3. Boundary conditions and numerical setup

In this study, a numerical model has been developed to study the force-indentation response on the living cell system during AFM, as depicted in Figure 1. The basal surface of the cell that is well adhered to the rigid substrate (e.g. cell culture dish) has been subjected to fixed boundary conditions, as the substrate is much harder than the cells. The cell surface in direct contact with the indenter is prescribed to zero stress and is restricted to follow the indenter profile. The rest of the cell surface, not in contact with the indenter is free to move. At different interfaces of the biological cell modeled as a cell body/nucleus composite material system, continuity boundary conditions have been imposed, i.e. the matrix and nucleus of living cells are perfectly bonded. External mechanical stimuli have been applied at the indenter in a vertically downward (axial) direction to quantify the reaction force and deformation induced within the cell under different loading conditions. Both static and dynamic indentations have been performed on the biological cell. Notably, indentations have been performed utilizing the most commonly used spherical and conical probes. The AFM indentation of the living cells has been simulated utilizing FEM based commercial COMSOL Multiphysics 5.5 software (COMSOL AB, Stockholm, 2019). A standard Lagrange (quadratic) shape function has been used to discretize the space domain for the physical field in our FEM analysis. The advantage of geometrical symmetry has been utilized by specifying the symmetric boundary conditions in the computational domain, wherever possible, to reduce the computational cost. The computational domain has been discretized using the spatial heterogeneous triangular mesh elements with higher mesh density at the indenter-cell interface. The mesh was generated by using COMSOL's built-in mesh generator and the mesh convergence analysis has been conducted by progressively refining the mesh until the absolute error for the reaction
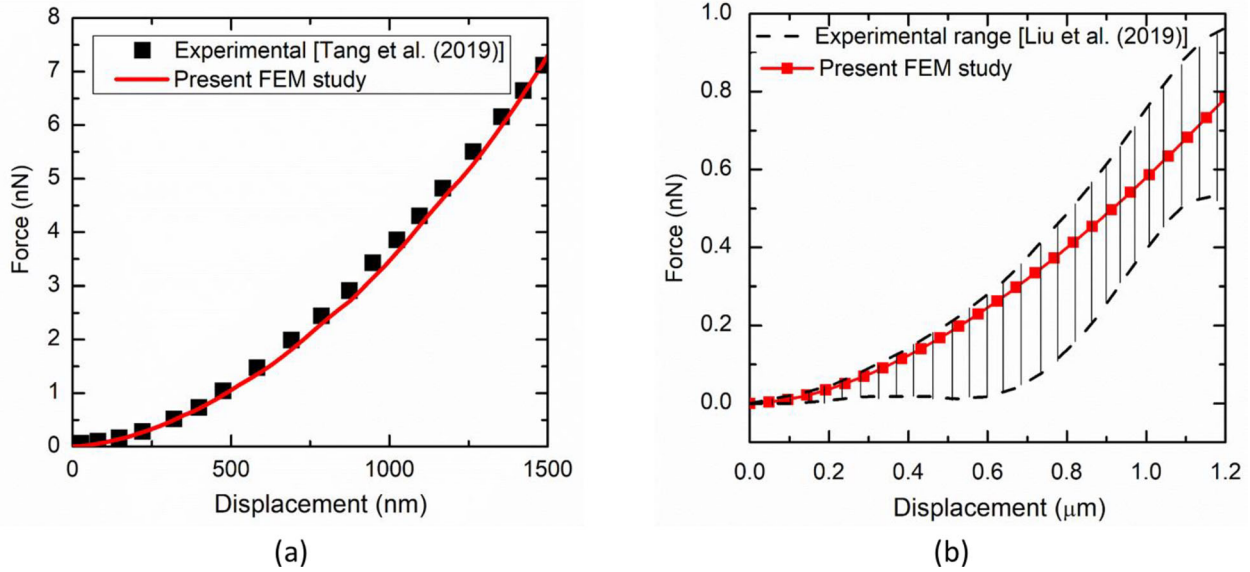
Figure 2. Comparison of the force-indentation curve of the developed FEM model against the AFM experimental results reported in (a) Tang et al. (2019) and (b) Liu et al. (2019).

force and von Mises stress becomes less than 0.5% for an additional refinement of the mesh. All simulations have been performed on a 64-bit 10 core Intel® Xeon® E5-2680 v2 @ 2.80 GHz processor.

3. Results and discussion

In the present study, a FEM-based numerical model has been developed to investigate the effect of nucleus auxeticity on the biological cell deformation during the AFM indentation under various loading conditions. Importantly, to account for nucleus auxeticity, a comparative analysis has been conducted to investigate the variations induced in the force indentation response considering cell nucleus with and without auxeticity. Furthermore, in most of the previously reported FEM studies on the AFM indentation, it is quite common to assume the entire cell as homogeneous, i.e. without any nucleus (Ladjal et al. 2009; Ding et al. 2017; Garcia and Garcia 2018b; Wang L et al. 2020). This assumption is very unrealistic with the heterogeneous multilayer nature of the biological cells. Hence, to address this issue we have developed a more realistic FEM model to quantify the mechanical response of the biological cells subjected to the AFM indentations by accounting for their intrinsic structural heterogeneity. Furthermore, parametric studies have been conducted to investigate the role of nucleus diameter, indenter shape and location on the stress distribution within the biological cell with an auxetic nucleus. The developed model fidelity and integrity have been evaluated by comparing the results

obtained from the present model with those available in the literature, incorporating similar geometrical configurations and loading profiles during the AFM indentation. The comparative analysis of the force-indentation curve of the present FEM study with the AFM experimental results of two recent studies (Liu et al. 2019; Tang et al. 2019) have been presented in Figure 2. As evident from Figure 2, the results predicted from the model proposed here are in good agreement with experiments reported in the previous studies and hence, it lends great confidence in the outcomes derived from the developed model.

The comparison of the predicted reaction force with indentation of the cell with and without auxetic nucleus has been presented in Figure 3(a). As evident from Figure 3(a), for smaller diameter nucleus (D = 3 μm), auxeticity has quite negligible influence on the force indentation response, and apparently, this deviation increases with an increase in the nucleus diameter. The force indentation response of the biological cell having 5 μm diameter auxetic nucleus ($\nu = -0.3$) is significantly higher as compared to the cell having a non-auxetic nucleus ($\nu = 0.3$). The comparison of the force-indentation curve on the size of the auxetic nucleus has been presented in Figure 3(b). It is evident from this figure that the cell nucleus size introduces the large differences in the predicted reaction force-indentation curves. The force-indentation curve is on the lower side if no nucleus is considered within the biological cell (i.e. the cell is homogeneous) and the introduction of heterogeneity, in terms of the nucleus, results in a
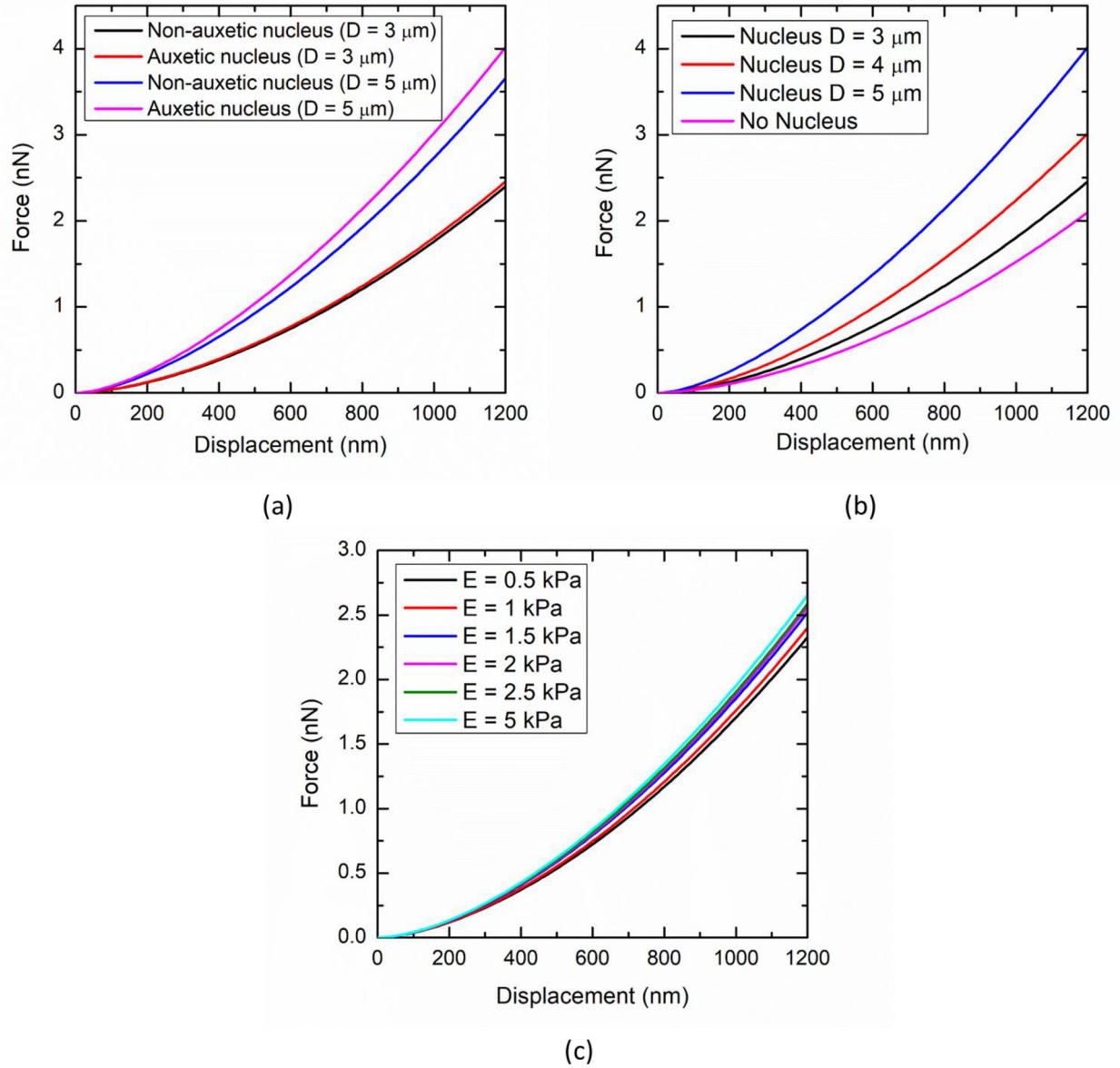
Figure 3. (Color online) Force – indentation curves demonstrating: (a) the comparison between auxetic and non-auxetic nucleus, (b) the effect of auxetic nucleus diameter, and (c) the effect of Young's modulus of elasticity of auxetic nucleus during the indentation of the cell body/nucleus composite biosystem.

corresponding increase in the force-displacement response. The effect of stiffness on the force-indentation profile of the biological cell with auxetic nucleus has been presented in Figure 3(c). Again, the force-indentation profile is on the lower side for the nucleus having Young's modulus of 0.5 kPa and is on the higher side for the nucleus having Young's modulus value of 5 kPa. Thus, the size and stiffness of the auxetic nucleus lead to a significant deviation in the force-displacement response during the AFM indentation.

Figure 4 presents the induced displacement and von Mises stress along the line perpendicular to the indentation direction that passes from the center of the nucleus, 3 μm in diameter. As evident from Figure 4, negligible variation prevails for the displacement induced due to the AFM indentation within the nucleus. However, the von Mises stress induced with an auxetic nucleus is considerably higher as compared to the von Mises stress induced with the non-auxetic nucleus. It is noteworthy to mention that von Mises stress, which is a scalar value computed from the stress tensor, represents the criterion for calculating whether the induced stress will cause the failure of the material or not (Singh and Melnik 2019; 2020a; Tang et al. 2019). Moreover, as mentioned earlier, this variation is going to increase with the increase in size (or volume) of the nucleus. The comparison of the von Mises contour plots among the auxetic and
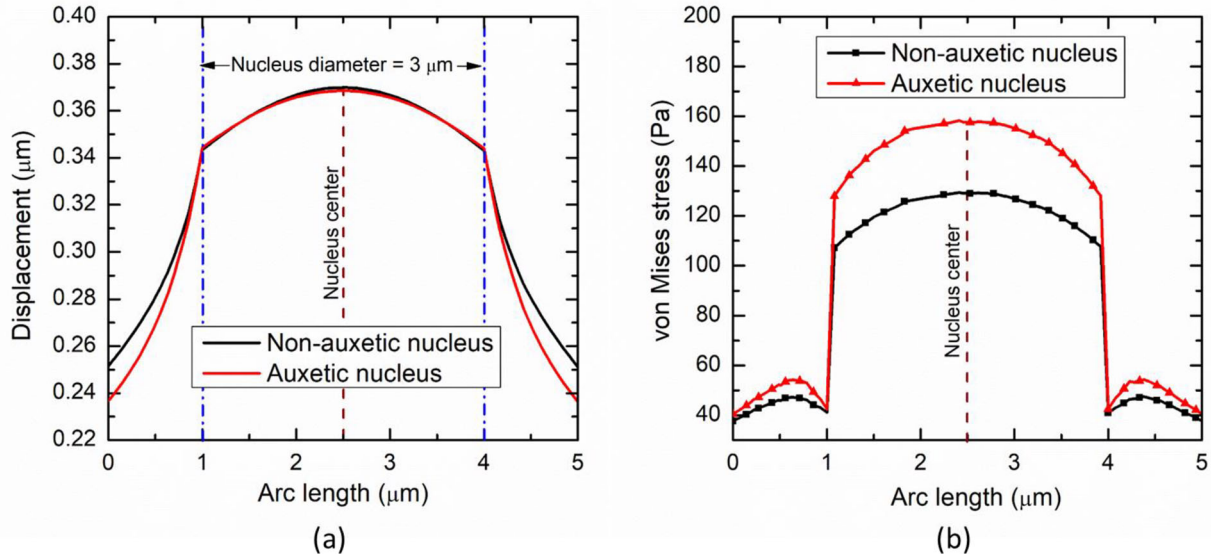
Figure 4. (Color online) (a) Displacement, and (b) von Mises stress distribution, at an indentation depth of 1.2 μm along the line perpendicular to the indentation direction that passes from the center of 3 μm diameter auxetic nucleus.
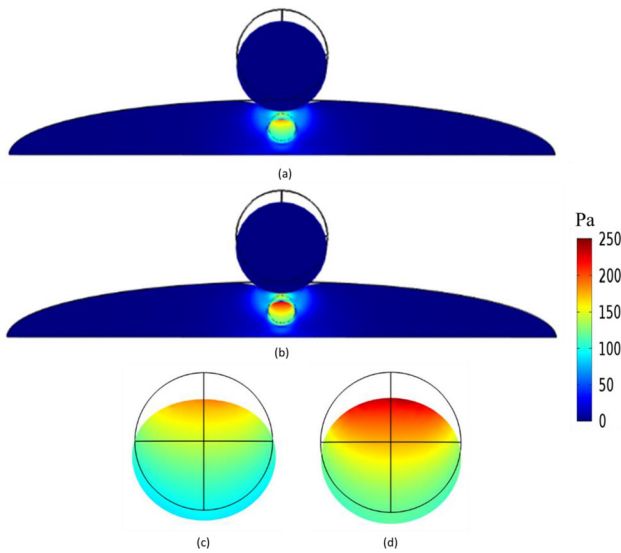

Figure 5. (Color online) Von Mises stress contour plots at an indentation depth of 1.2 μm for: (a,c) non-auxetic and (b,d) auxetic nucleus.

non-auxetic nucleus at the indentation depth of 1.2 μm has been presented in Figure 5. It can be seen from Figure 5 that the von Mises stress induced with the auxetic nucleus in the MDA-MB-231 living cell is on the higher side as compared to the non-auxetic nucleus. As expected, the region of cell-matrix sandwiched between the spherical indenter and the cell nucleus is severely deformed. Furthermore, the upper region of the nucleus experiences higher deformation as compared to the lower portion, resulting in the concentration of higher von Mises stresses in the upper region, as presented in Figure 5(c)–(d).

The effect of indenter location from the center of the auxetic nucleus on the force-displacement response during AFM has also been quantified in the present study. Importantly, four different locations of the indenter have been considered, viz., indenter directly on the top of the underlying nucleus (i.e. perfectly aligned indentation), indenter center offset from the nucleus center by 1 μm, 2 μm and 5 μm that represents the misaligned indentation (Tang et al. 2019). The displacement and von Mises stress distributions for different locations of indenter with respect to the auxetic nucleus center have been presented in Figures 6 and 7, respectively. As evident from these figures, the force indentation response during AFM of a biological cell considered here is quite sensitive to the location of the indenter. Symmetric distribution of both the displacement and von Mises stress has been observed for perfectly aligned indentation. Even a small amount of indenter offset from the auxetic nucleus center results in asymmetric variations of displacement and von Mises stress within the cell. Moreover, both the displacement and von Mises stress are significantly greater than in a perfectly aligned case as compared to the misaligned case. This can be attributed to the fact that for the perfectly aligned case, the indenter could completely detect the existence of the nucleus as a hard inclusion, and thus both the nucleus and surrounding matrix are highly compressed. For misaligned indenter, most of the deformation induced due to the AFM indentation is absorbed by the weaker matrix region, thereby generating a slightly tilted contact surface and asymmetric
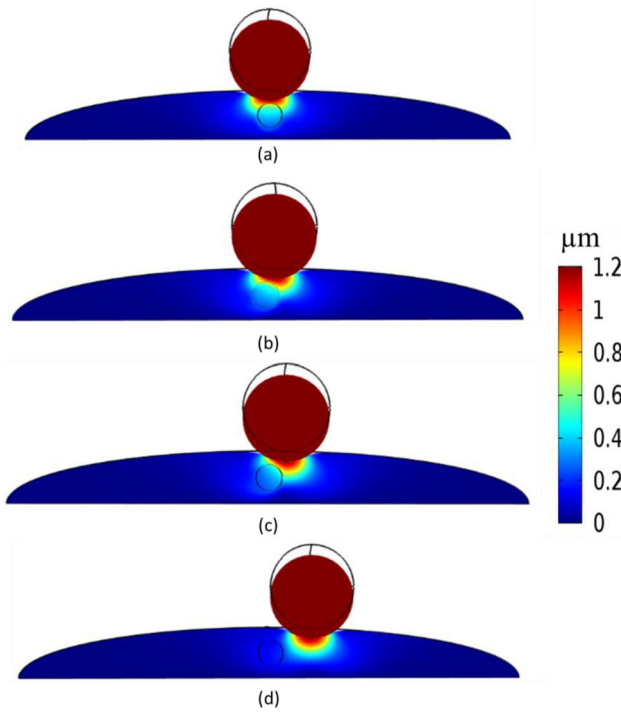
Figure 6. (Color online) Displacement distributions induced within the biological cell during the AFM indentation of the cell body/nucleus composite biosystem with spherical indenter for: (a) perfectly aligned indentation, and misaligned indentation with an offset value of: (b) 1 μm, (c) 2 μm, and (d) 5 μm between the nucleus and the indenter at an indentation depth of 1.2 μm.

Figure 7. (Color online) Von mises stress distributions induced within the biological cell during the AFM indentation of the cell body/nucleus composite biosystem with spherical indenter for: (a) perfectly aligned indentation, and misaligned indentation with an offset value of: (b) 1 μm, (c) 2 μm, and (d) 5 μm between the nucleus and the indenter at an indentation depth of 1.2 μm.

variations that could push the nucleus away from the surface where the force is applied from the indenter tip. The force indentation profile for different indentation positions has been presented in Figure 8. It can be seen from Figure 8 that the maximum reaction force has been obtained for the perfectly aligned indenter. The offset of the indenter from the auxetic nucleus center results in a much lower reaction force, as is evident from Figure 8.

The comparison of the von Mises stress distributions for the non-auxetic and auxetic nucleus under the AFM indentation with a conical probe has been presented in Figures 9(a) and (b). As evident from these figures, for the case of the auxetic nucleus the top surface of the nucleus experiences higher von Mises stress in comparison to the non-auxetic nucleus. The line graph of von Mises stress along the line that passes from the nucleus center and is perpendicular to the direction of indentation has been presented in Figure 9(c). Again, concurrent with the results obtained with spherical indenter, the von Mises stress induced due to the AFM indentation utilizing conical probe in the auxetic nucleus is higher as compared to the non-auxetic nucleus. Moreover,
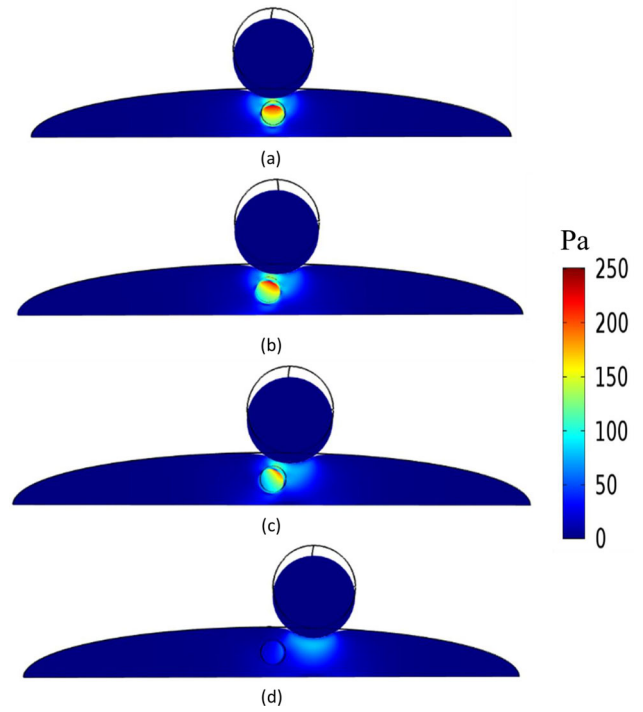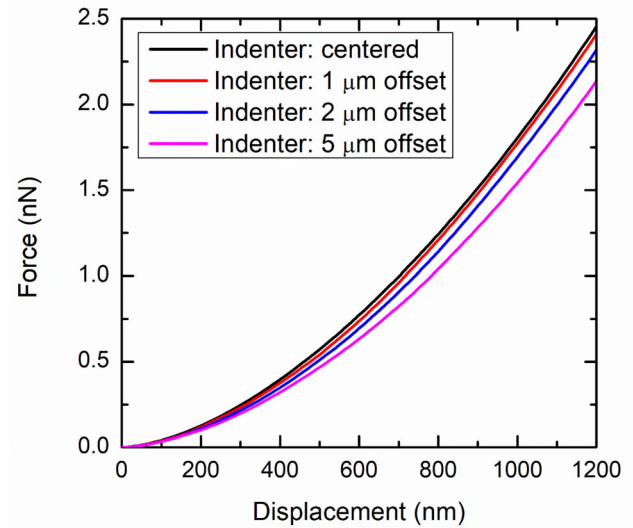

Figure 8. (Color online) Force-indentation response of the biological cell with auxetic nucleus during the AFM indentation with a perfectly aligned setup and various offset value between the nucleus and the indenter in the misaligned setup.

the maximum value of the induced von Mises stress with spherical indenter was more than three times higher as compared to the conical indenter under the
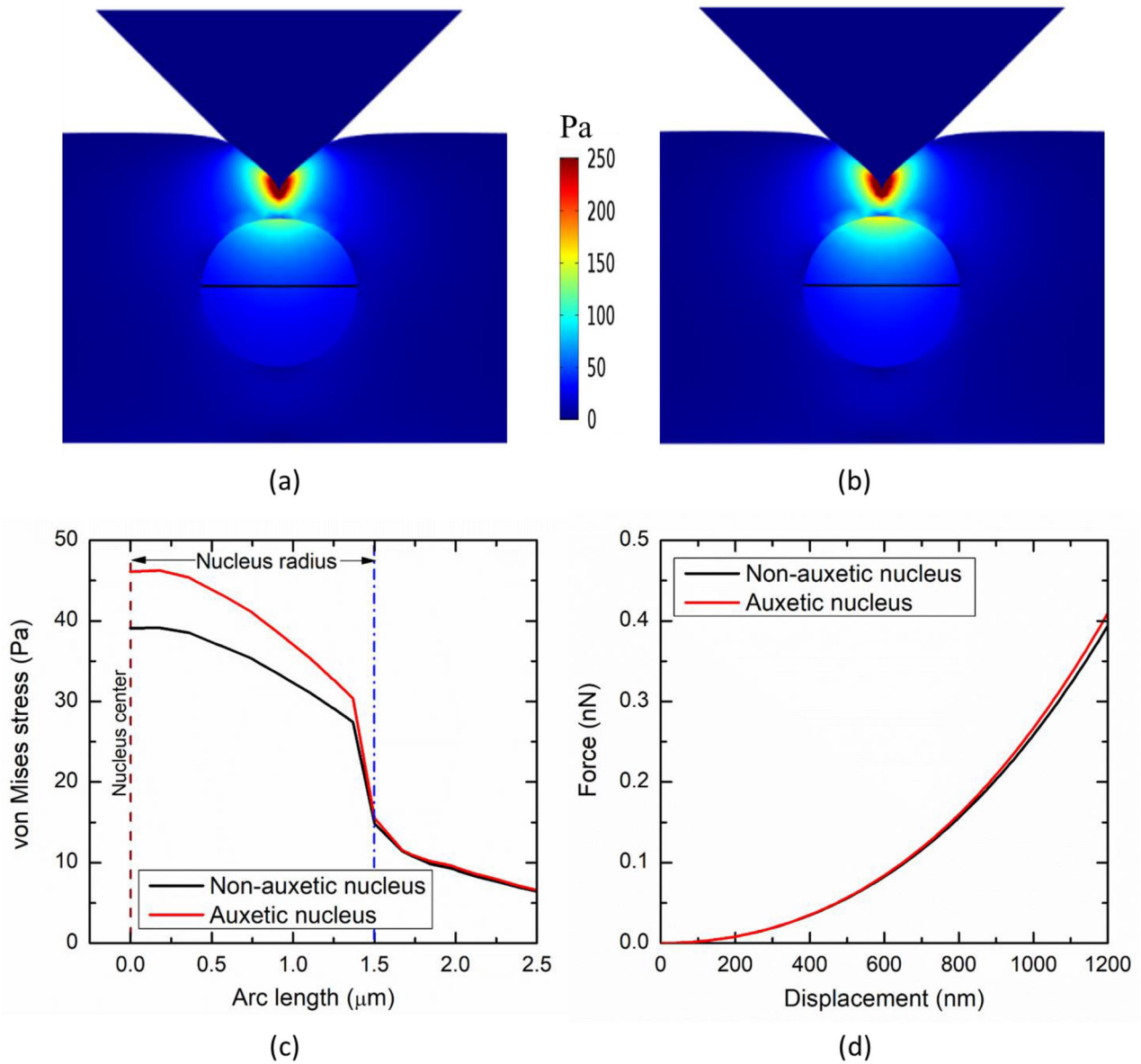
Figure 9. (Color online) Von Mises stress contour plots of AFM indentation of biological cell with conical probe at an indentation depth of 1.2 μm for: (a) non-auxetic and (b) auxetic nucleus. (c) von Mises stress distribution along the line perpendicular to the indentation direction that passes from the center of auxetic nucleus at an indentation depth of 1.2 μm. (d) force-indentation response of the biological cell with non-auxetic and auxetic nucleus during the AFM indentation with a conical indenter.

application of the same applied force. This can be attributed to the fact that as compared to the conical probe, the spherical indenter has more contact surface with the biological cell that leads to a much highly stressed nucleus and the surrounding matrix. The comparison of the reaction forces obtained for auxetic and non-auxetic nucleus with the AFM indentation utilizing a conical probe has been presented in Figure 9(d). It can be seen from Figure 9(d) that the reaction force obtained for an auxetic nucleus is slightly higher as compared to the non-auxetic nucleus. Again, this variation is expected to increase with increasing the diameter of the nucleus.

In the present study, the effects of nucleus auxeticity on the mechanical behavior of stem cells have also been quantified under the triangular and trapezoidal loading-unloading profiles during the AFM indentation. Motivated by Katti and Katti (2017), both the loading and unloading periods for trapezoidal and triangular profiles have been assumed to be 1 s keeping the maximum indentation depth to be 1.2 μm (same as for the previous part of this study). The comparative analysis of the von Mises stress induced at the tip of the spherical indenter for the auxetic and non-auxetic nucleus has been presented in Figure 10. As evident from Figure 10, the von Mises stress induced for
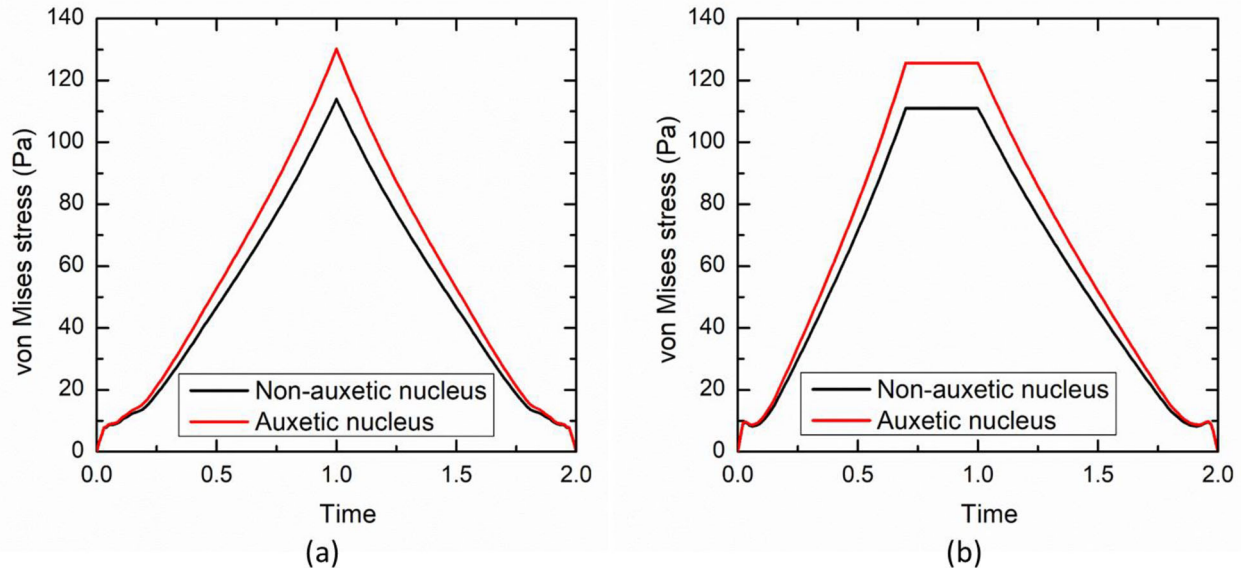
Figure 10. (Color online) Von Mises stress distribution at the tip of spherical indenter for the auxetic and non-auxetic nucleus utilizing: (a) triangular and (b) trapezoidal loading-unloading profiles during AFM indentation.

the case of the auxetic nucleus is significantly higher as compared to the non-auxetic nucleus for both the triangular and trapezoidal profiles. At the peak loading time of 1 s, the von Mises stress induced with auxetic nucleus has been found 14.20% higher for a triangular profile and 13.23% higher for a trapezoidal profile as compared to the non-auxetic nucleus. The results of von Mises stress distribution for dynamic indentation of the biological cell along the line perpendicular to the indentation direction that passes from the center of 3 μm diameter nucleus have been presented in Figure 11 for both trapezoidal and triangular loading-unloading profiles. It can be seen from Figure 11 that the variation in von Mises stress for auxetic and non-auxetic nuclei is significantly lower initially and it increases with passage of time.

Furthermore, previous studies have demonstrated that the cytoplasmic structure of biological cell possess viscoelastic behavior (Fallqvist et al. 2016; Unnikrishnan et al. 2016). This effect has been accounted for in the present study by modeling the cytoplasm as a viscoelastic material. Notably, viscoelastic effect has been incorporated by adding two generalized Maxwell branches (with energy factor of 10 and relaxation times of 0.5 s and 50 s for the first and second branch, respectively) in the strain-energy density function of the neo-Hookean model of cytoplasm, as presented in section 2.2. Motivated by Fallqvist et al. (2016), the spherical indenter during AFM has been prescribed with a velocity of 0.1 μm/s, until the total vertical displacement is 1.2 μm and subsequently the indenter position is held fixed for the

rest of the time till 30 s. The vertical indenter force exerted on the spherical indenter during AFM has been presented in Figure 12(a) for biological cells with auxetic and non-auxetic nuclei. As evident from this figure, the exerted force is marginally higher for auxetic nucleus as compared to non-auxetic nucleus. The von Mises stresses induced at the center of nucleus for non-auxetic and auxetic nuclei has been presented in Figure 12(b). It is observed from Figure 12(b) that the temporal variation of the von Mises stress is significantly higher for the cell with auxetic nucleus as compared to cell with non-auxetic nucleus. Moreover, the von Mises stress increases abruptly in first few seconds, attains a peak (that corresponds to the maximum displacement of the indenter (i.e. 1.2 μm)) and then declines. The effect of nucleus diameter on the temporal variation of the von Mises stresses induced at the center of nucleus for cell with auxetic nucleus has been presented in Figure 12(c). As evident from Figure 12(c), the higher the nucleus diameter is, the lower will be the von Mises stresses induced at the center of the nucleus. This can be attributed to the fact that the higher the nucleus, the higher will be the stiffness of nucleus that will provide hindrance to the concentration of the stresses at the center of nucleus. The von Mises stress distributions for different times (viz., 1.2 s (corresponding to the maximum indenter displacement of 1.2 μm), 5 s and 30 s) have been presented in Figure 13 for a biological cell with non-auxetic and auxetic nuclei.

The developed model successfully captures the mechanical behavior of cells induced due to the
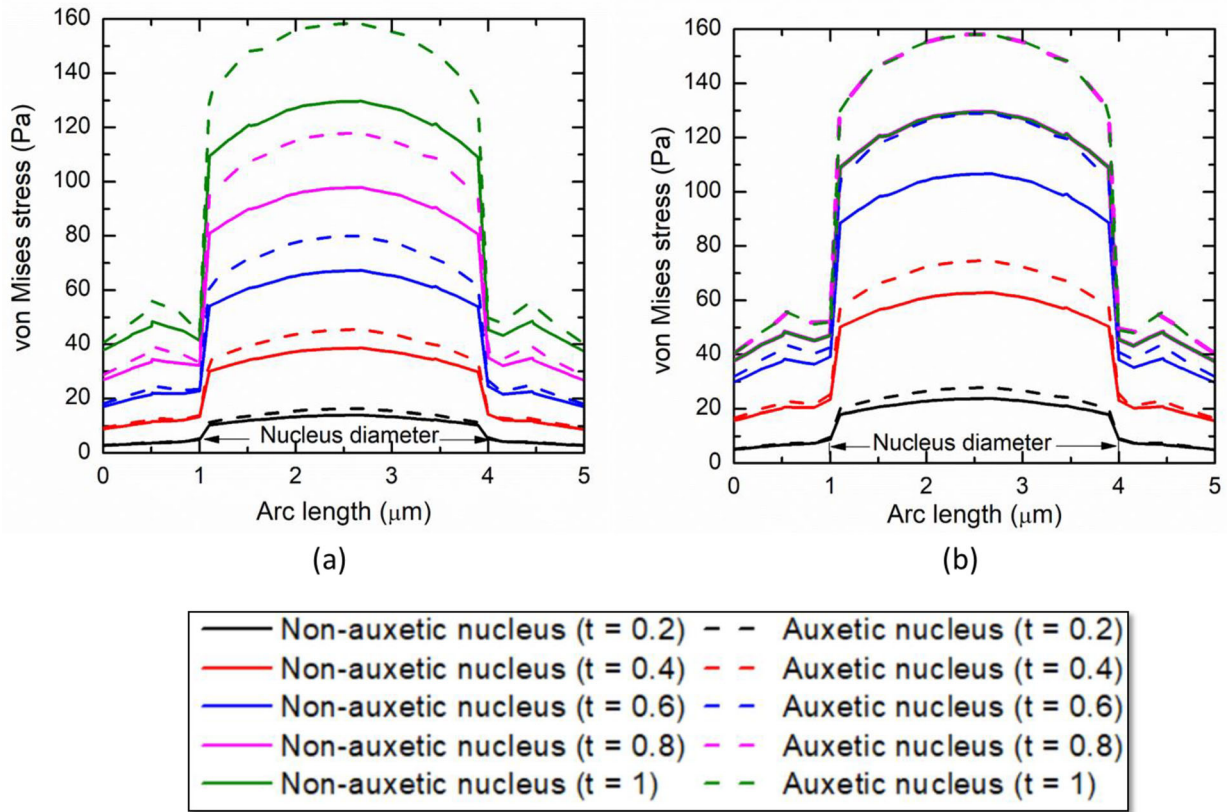
Figure 11. (Color online) Comparison between the von Mises stress distribution along the line perpendicular to the indentation direction that passes from the center of non-auxetic and auxetic nucleus for different time steps utilizing: (a) triangular and (b) trapezoidal loading-unloading profiles during AFM indentation.

highly unique auxetic property of the nucleus of the self-renewing stem cell during indentation tests (Fuchs and Chen 2013; Chang 2020; Xu et al. 2020). Apart from other applications, these properties are thought to be the key to a number of new regenerative therapies. The reported results of the model could pave a way forward for our better understanding of the dynamic structural, mechanical and biophysical changes occurring due to nucleus auxeticity. Notably, this numerical study highlighted that the biological cell with an auxetic nucleus behaves differently as compared to the cell with a non-auxetic nucleus when exposed to mechanical stimuli. The volume change of a cell with an auxetic nucleus would be completely different from that of a non-auxetic nucleus. This variation could lead to abrupt changes in the diffusion of the soluble molecules across the nucleus and eventually could control the differentiation process in the stem cell (Hodgson et al. 2017). Further studies are required to fully elucidate the role of auxeticity in the differentiation and regeneration of stem cells that could provide a significant inspiration to the field of regenerative medicine and tissue engineering. The developed model can be further extended by

including the individual cytoskeleton elements (microtubules, intermediate and actin filaments) (Keeling et al. 2017; Singh and Melnik 2020b, 2020c) to further improve the understanding of the mechanical behavior of biological cells subjected to external stimuli and linking it to the mechanotransduction process that is difficult to quantify using experimental techniques at such small scales. A better understanding of the auxeticity within living materials could also assist in designing and engineering new auxetic meta-biomaterials that aim at achieving a unique combination of mechanical, mass transport and biological properties by optimizing topological designs generated utilizing 3 D/4D printing and other additive manufacturing technologies (HM Kolken and Zadpoor 2017; Zadpoor 2019; H Kolken et al. 2020; Zadpoor 2020).

4. Conclusion

Auxeticity has been known in biosystems for more than a century, e.g. in the skin of aquatic salamander, cow teat skin, and cat skin. This list can be continued to include cancellous bones from the proximal tibial epiphysis, human Achilles tendons, human Peroneus
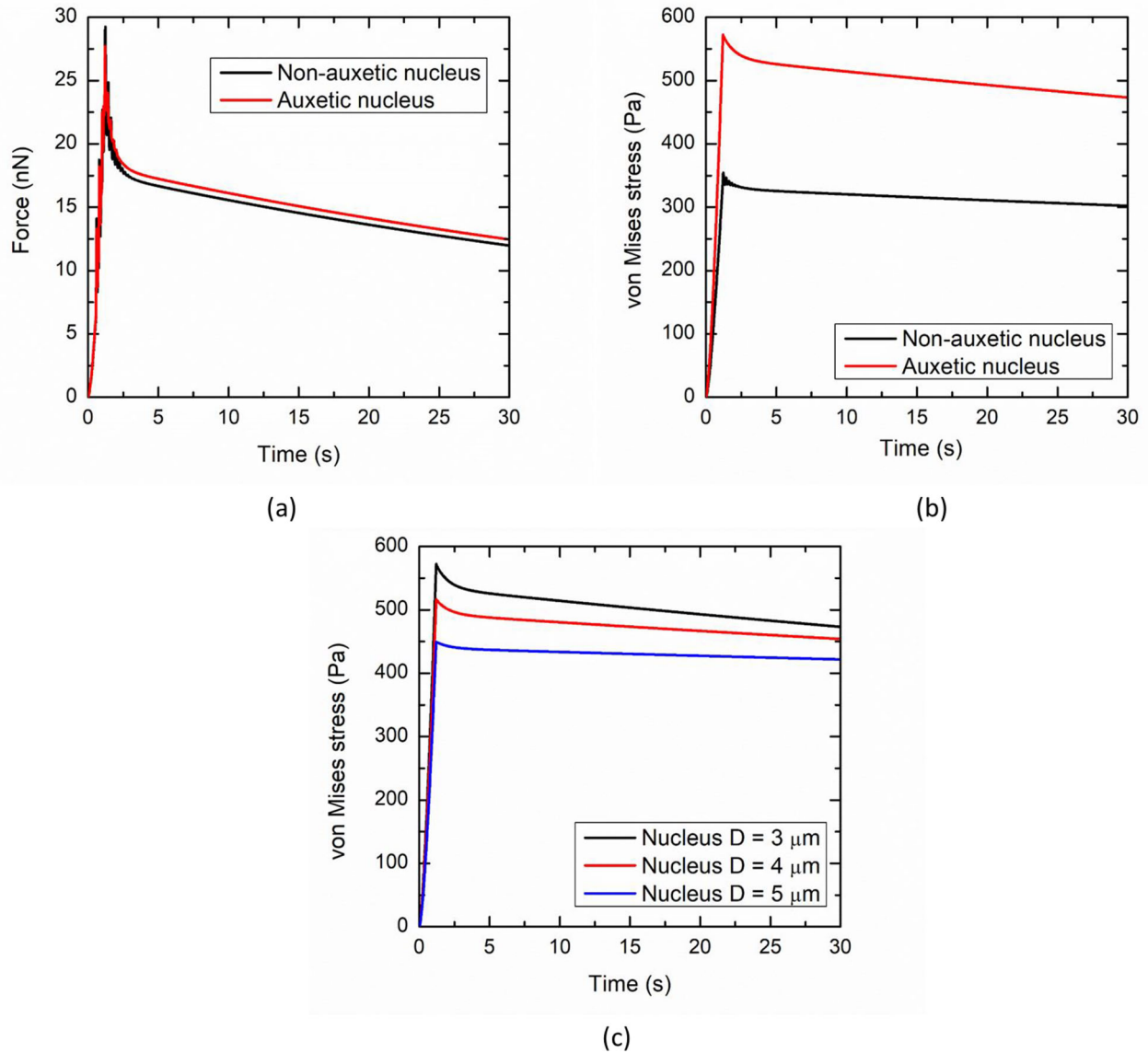
Figure 12. (Color online) Effect of viscoelastic cytoplasm on: (a) force − indentation curves of auxetic and non-auxetic nucleus, (b) von Mises stresses for auxetic and non-auxetic nucleus quantified at the center of nucleus, (c) von Mises stress distributions for different diameters of auxetic nucleus.

brevis, porcine and ovine deep flexor tendons, bovine arteries, intervertebral disc of cow and pigs (Santulli and Langella 2016; Mardling et al. 2020). The interest to auxeticity has also been growing in the context of deployable biomimicking structures and sustainable biosystem-based design (Santulli and Langella 2016; Zhang et al. 2020). Inspired from this highly unique auxetic behavior found in nature, man-made auxetic structures have recently sparked significant interest among designers, architects and researchers. The advances in 3 D/4D bioprinting, including such areas as tissue engineering, and robotic fabrication technologies have also provided a massive boost to this field of creation of new meta-materials (Papadopoulou et al. 2017). Further, due to their superior compressive

strength and shear stiffness, auxetic materials have been widely used for bioprostheses and artery stents. Also, auxetic scaffolds (i.e. scaffolds that can display negative Poisson's ratio) are used in vascular engineering to prevent blockages by allowing the widening of blood vessels due to induced compressive stresses with blood flow (Song et al. 2018). As we mentioned earlier, it has also been found that the nucleus of embryonic stem cells becomes auxetic when they differentiate and are in the transition period leaving the state of pluripotency (Pagliara et al. 2014; Tripathi and Menon 2019). This is an extraordinary example of the auxeticity in biosystems. Previous experiments have confirmed that the embryonic stem cell nuclei become smaller (instead of becoming fatter) by
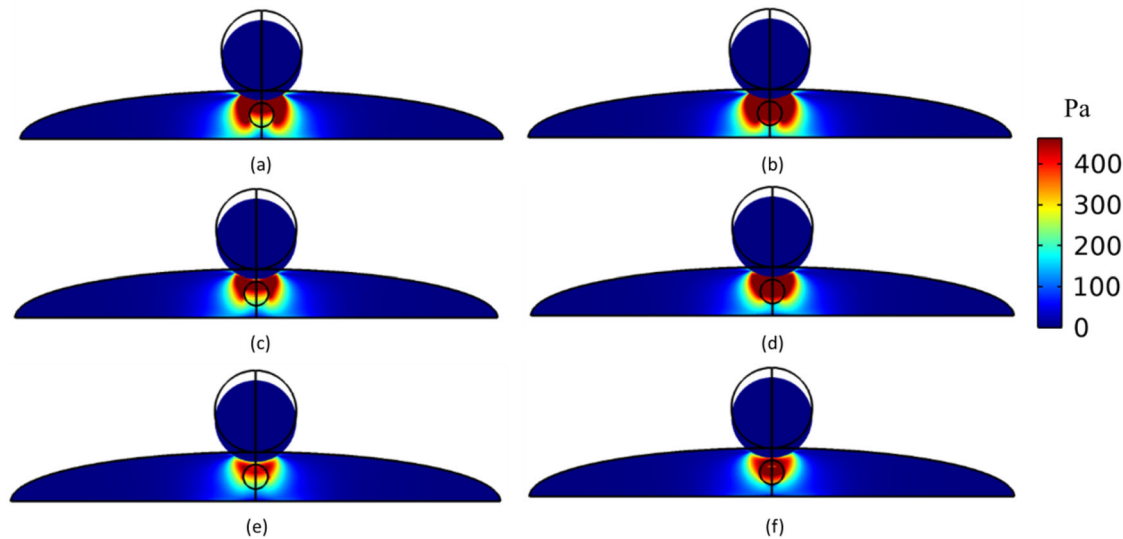
Figure 13. (Color online) Von Mises stress distributions induced within the biological cell with viscoelastic cytoplasm for: (a, c, e) non-auxetic nucleus and (b, d, f) auxetic nucleus. (a–b) at 1.2 s, (c–d) at 5 s, and (e–f) at 30 s.

5–10% in cross-section when compressed with the AFM indenter to a level of 2 μm, thus possessing a highly unique property of negative Poisson's ratio (Pagliara et al. 2014; Tripathi and Menon 2019). It has also been reported that the auxeticity originates naturally in the biophysical properties of the embryonic stem cell nucleus due to the significant global decondensation of chromatin and not due to the extranuclear environment. Similar auxetic behavior has also been reported in the nucleus of the oligodendrocyte progenitor cell (a subtype of glial cells in the central nervous system) (UKRI 2020). It is noteworthy to mention that, as far as it is currently known, the nuclei of all other biological cells possess a positive Poisson's ratio (Pagliara et al. 2014; Hodgson et al. 2017). A recent finding has also depicted the role of cytoskeletal networks (actin, myosin, tubulin, and vimentin) in modulating nuclear shape and mechanics (Keeling et al. 2017). In particular, this study reported that cytoskeletal networks except actin contribute to the nucleus stiffening. Also, it was found that actin and vimentin are the strongest contributors in modulating Poisson's ratio, while vimentin and myosin have the largest influence on the nuclear volume. Thus, a proper understanding of the underlying auxetic mechanism in the living material would significantly assist in designing new meta-biomaterials that could mimic the natural properties of biological tissue and would have strong and positive implications in regenerative medicine, tissue engineering, drug discovery and sustainable design areas.

In this contribution, we have emphasized the role of auxeticity in both living and man-made biosystems. Our special attention has been given to the role of the nucleus auxeticity on the mechanical behavior of the embryonic stem cells in the transitional state which has been demonstrated on a number of examples. A FEM model of the heterogeneous embryonic stem cells has been developed to simulate their mechanical behavior under distinct mechanical stimuli. A comparative analysis has been conducted to quantify the deviations induced in the force-displacement response during the AFM indentation of the biological cell with auxetic and non-auxetic nuclei. The magnitude of the induced von Mises stresses with auxetic nucleus has been found to be far pronounced as compared to the non-auxetic nucleus. This variation increases with an increase in the size of the nucleus. The results reported in this study would assist in our better understanding of the auxetic behavior in the living materials that could lead to new frontiers in the novel geometrical design of meta-biomaterials with tailored properties utilizing 3 D/4D printing technologies. With the development of auxetic cellular networks, based on soft biological tissues, and our further insight into the autophagy process of stem cell systems, this research is a first step in the quantification of auxeticity effects for their applications in new regenerative and tissue engineering technologies, among other areas.

Acknowledgements

Disclosure statement

No potential conflict of interest was reported by the authors.

ORCID

Sundeep Singh ⓘ http://orcid.org/0000-0002-8342-1622
Roderick Melnik ⓘ http://orcid.org/0000-0002-1560-6684

References

Addae-Mensah KA, Wikswo JP. 2008. Measurement techniques for cellular biomechanics in vitro. Exp Biol Med (Maywood). 233(7):792–809.

Barreto S, Clausen CH, Perrault CM, Fletcher DA, Lacroix D. 2013. A multi-structural single cell model of force-induced interactions of cytoskeletal components. Biomaterials. 34(26):6119–6126.

Basoli F, Giannitelli SM, Gori M, Mozetic P, Bonfanti A, Trombetta M, Rainer A. 2018. Biomechanical characterization at the cell scale: present and prospects. Front Physiol. 9:1449.

Bonilla M, Stokes J, Gidley M, Yakubov G. 2015. Interpreting atomic force microscopy nanoindentation of hierarchical biological materials using multi-regime analysis. Soft Matter. 11(7):1281–1292.

Cabras L, Brun M. 2014. Auxetic two-dimensional lattices with Poisson's ratio arbitrarily close to −1. Proc Roy Soc A Math Phys Eng Sci. 470(2172):20140538.

Chang NC. 2020. Autophagy and stem cells: self-eating for self-renewal. Front Cell Dev Biol. 8:138.

COMSOL AB, Stockholm. 2019. COMSOL Multiphysics®v. 5.5. www.comsol.com.

Dagro A, Rajbhandari L, Orrego S, Kang SH, Venkatesan A, Ramesh KT. 2019. Quantifying the local mechanical properties of cells in a fibrous three-dimensional microenvironment. Biophys J. 117(5):817–828.

Dagro AM, Ramesh K. 2019. Nonlinear contact mechanics for the indentation of hyperelastic cylindrical bodies. Mech Soft Mater. 1(1):7.

Digiuni S, Berne-Dedieu A, Martinez-Torres C, Szecsi J, Bendahmane M, Arneodo A, Argoul F. 2015. Single cell wall nonlinear mechanics revealed by a multiscale analysis of AFM force-indentation curves. Biophys J. 108(9):2235–2248.

Ding Y, Wang J, Xu G-K, Wang G-F. 2018. Are elastic moduli of biological cells depth dependent or not? Another explanation using a contact mechanics model with surface tension. Soft Matter. 14(36):7534–7541.

Ding Y, Xu G-K, Wang G-F. 2017. On the determination of elastic moduli of cells by AFM based indentation. Sci Rep. 7:45575.

Domaschke S, Morel A, Fortunato G, Ehret AE. 2019. Random auxetics from buckling fibre networks. Nat Commun. 10(1):1–8.

Efremov YM, Wang W-H, Hardy SD, Geahlen RL, Raman A. 2017. Measuring nanoscale viscoelastic parameters of cells directly from AFM force-displacement curves. Sci Rep. 7(1):1–14.

Fallqvist B, Fielden ML, Pettersson T, Nordgren N, Kroon M, Gad AK. 2016. Experimental and computational assessment of F-actin influence in regulating cellular stiffness and relaxation behavior of fibroblasts. J Mech Behav Biomed Mater. 59:168–184.

Fuchs E, Chen T. 2013. A matter of life and death: self-renewal in stem cells. EMBO Rep. 14(1):39–48.

Garcia PD, Garcia R. 2018a. Determination of the elastic moduli of a single cell cultured on a rigid support by force microscopy. Biophys J. 114(12):2923–2932.

Garcia PD, Garcia R. 2018b. Determination of the viscoelastic properties of a single cell cultured on a rigid support by force microscopy. Nanoscale. 10(42):19799–19809.

Garcia PD, Guerrero CR, Garcia R. 2020. Nanorheology of living cells measured by AFM-based force-distance curves. Nanoscale. 12(16):9133–9143.

Gatt R, Vella Wood M, Gatt A, Zarb F, Formosa C, Azzopardi KM, Casha A, Agius TP, Schembri-Wismayer P, Attard L, et al. 2015. Negative Poisson's ratios in tendons: An unexpected mechanical response. Acta Biomater. 24:201–208.

Haase K, Pelling AE. 2015. Investigating cell mechanics with atomic force microscopy. J R Soc Interface. 12(104):20140970.

Hertz H. 1882. Ueber die Berührung fester elastischer Körper. Journal Für Die Reine Und Angewandte Mathematik. 1882(92):156–171.

Hodgson AC, Verstreken CM, Fisher CL, Keyser UF, Pagliara S, Chalut KJ. 2017. A microfluidic device for characterizing nuclear deformations. Lab Chip. 17(5):805–813.

Holzapfel GA, Gasser TC, Ogden RW. 2000. A new constitutive framework for arterial wall mechanics and a comparative study of material models. J Elast Phys Sci Solid. 61(1-3):1–48.

Kasas S, Gmur T, Dietler G. 2017. Finite-element analysis of microbiological structures. In The world of nano-biomechanics. Amsterdam, Netherlands: Elsevier; p. 199–218.

Katti DR, Katti KS. 2017. Cancer cell mechanics with altered cytoskeletal behavior and substrate effects: A 3D finite element modeling study. J Mech Behav Biomed Mater. 76:125–134.

Keeling MC, Flores LR, Dodhy AH, Murray ER, Gavara N. 2017. Actomyosin and vimentin cytoskeletal networks regulate nuclear shape, mechanics and chromatin organization. Sci Rep. 7(1):1–14.

Kolken H, Lietaert K, van der Sloten T, Pouran B, Meynen A, Van Loock G, Weinans H, Scheys L, Zadpoor AA. 2020. Mechanical performance of auxetic meta-biomaterials. J Mech Behav Biomed Mater. 104:103658.

Kolken HM, Zadpoor A. 2017. Auxetic mechanical metamaterials. RSC Adv. 7(9):5111–5129.

Krieg M, Fläschner G, Alsteens D, Gaub BM, Roos WH, Wuite GJ, Gaub HE, Gerber C, Dufrêne YF, Müller DJ.

2019. Atomic force microscopy-based mechanobiology. Nat Rev Phys. 1(1):41–57.

Krishnaswamy JA, Buroni FC, Melnik R, Rodriguez-Tembleque L, Saez A. 2020. Design of polymeric auxetic matrices for improved mechanical coupling in lead-free piezocomposites. Smart Mater Struct. 29(5):054002.

Krishnaswamy JA, Buroni FC, Melnik R, Rodriguez-Tembleque L, Saez A. 2021. Multiscale design of nanoengineered matrices for lead-free piezocomposites: Improved performance via controlling auxeticity and anisotropy. Compos Struct. 255:112909.

Ladjal H, Hanus JL, Pillarisetti A, Keefer C, Ferreira A, Desai JP. 2009. Atomic force microscopy-based single-cell indentation: Experimentation and finite element simulation. IEEE/RSJ International Conference on Intelligent Robots and Systems, 2009: IEEE.

Lammerding J. 2011. Mechanics of the nucleus. Compr Physiol. 1(2):783–807.

Li X, Wang Q, Yang Z, Lu Z. 2019. Novel auxetic structures with enhanced mechanical properties. Extreme Mech Lett. 27:59–65.

Liu Y, Mollaeian K, Ren J. 2019. Finite element modeling of living cells for AFM indentation-based biomechanical characterization. Micron. 116:108–115.

Mardling P, Alderson A, Jordan-Mahy N, Le Maitre CL. 2020. The use of auxetic materials in tissue engineering. Biomater Sci. 8(8):2074–2083.

Melnik RV, Wei X, Moreno–Hagelsieb G. 2009. Nonlinear dynamics of cell cycles with stochastic mathematical models. J Biol Syst. 17(03):425–460.

Pagliara S, Franze K, McClain CR, Wylde GW, Fisher CL, Franklin RJ, Kabla AJ, Keyser UF, Chalut KJ. 2014. Auxetic nuclei in embryonic stem cells exiting pluripotency. Nat Mater. 13(6):638–644.

Papadopoulou A, Laucks J, Tibbits S. 2017. Auxetic materials in design and architecture. Nat Rev Mater. 2(12):1–3.

Ren X, Das R, Tran P, Ngo TD, Xie YM. 2018. Auxetic metamaterials and structures: a review. Smart Mater Struct. 27(2):023001.

Saeed M, Weihs D. 2019. Finite element analysis reveals an important role for cell morphology in response to mechanical compression. Biomech Model Mechanobiol. 19:1155–1164.

Santulli C, Langella C. 2016. Study and development of concepts of auxetic structures in bio-inspired design. IJSDES. 3(1):20–37.

Singh S, Krishnaswamy JA, Melnik R. 2020. Biological cells and coupled electro-mechanical effects: The role of organelles, microtubules, and nonlocal contributions. J Mech Behav Biomed Mater. 110:103859.

Singh S, Melnik R. 2019. Coupled thermo-electro-mechanical models for thermal ablation of biological tissues and heat relaxation time effects. Phys Med Biol. 64(24):245008.

Singh S, Melnik R. 2020a. Computational modeling of cardiac ablation incorporating electrothermomechanical interactions. J Eng Sci Med Diagnos Ther. 3(4):041004.

Singh S, Melnik R. 2020b. Coupled electro-mechanical behavior of microtubules. International Work-Conference on Bioinformatics and Biomedical Engineering; Springer.

Singh S, Melnik R. 2020c. Microtubule biomechanics and the effect of degradation of elastic moduli. International Conference on Computational Science; Springer.

Sneddon IN. 1965. The relation between load and penetration in the axisymmetric Boussinesq problem for a punch of arbitrary profile. Int J Eng Sci. 3(1):47–57.

Song L, Ahmed MF, Li Y, Zeng C, Li Y. 2018. Vascular differentiation from pluripotent stem cells in 3-D auxetic scaffolds. J Tissue Eng Regen Med. 12(7):1679–1689.

Soyarslan C, Blümer V, Bargmann S. 2019. Tunable auxeticity and elastomechanical symmetry in a class of very low density core-shell cubic crystals. Acta Mater. 177:280–292.

Tang G, Galluzzi M, Zhang B, Shen Y-L, Stadler FJ. 2019. Biomechanical heterogeneity of living cells: comparison between atomic force microscopy and finite element simulation. Langmuir. 35(23):7578–7587.

Tatara Y. 1989. Extensive theory of force-approach relations of elastic spheres in compression and in impact.

Tripathi K, Menon GI. 2019. Chromatin compaction, auxeticity, and the epigenetic landscape of stem cells. Phys Rev X. 9(4):041020.

UKRI. 2020. The auxetic nucleus: nuclear mechanotransduction and its role in regulating stem cell differentiation. [accessed Nov, 2020]. https://gtr.ukri.org/projects?ref=BB%2FM008827%2F1#/tabOverview.

Unnikrishnan GU, Unnikrishnan VU, Reddy J. 2016. Contribution of material properties of cellular components on the viscoelastic, stress-relaxation response of a cell during AFM indentation. Int J Comput Methods Eng Sci Mech. 17(3):137–142.

Wang K, Chang Y-H, Chen Y, Zhang C, Wang B. 2015. Designable dual-material auxetic metamaterials using three-dimensional printing. Mater Des. 67:159–164.

Wang Z, Luan C, Liao G, Liu J, Yao X, Fu J. 2020. Progress in auxetic mechanical metamaterials: structures. Adv Eng Mater. 22(10):2000312.

Wang L, Tian L, Wang Y, Zhang W, Wang Z, Liu X. 2020. Determination of viscohyperelastic properties of tubule epithelial cells by an approach combined with AFM nanoindentation and finite element analysis. Micron. 129:102779.

Warner JJ, Gillies AR, Hwang HH, Zhang H, Lieber RL, Chen S. 2017. 3D-printed biomaterials with regional auxetic properties. J Mech Behav Biomed Mater. 76:145–152.

Xu Y, Zhang Y, García-Cañaveras JC, Guo L, Kan M, Yu S, Blair IA, Rabinowitz JD, Yang X. 2020. Chapter one-mediated autophagy regulates the pluripotency of embryonic stem cells. Science. 369(6502):397–403.

Zadpoor AA. 2019. Mechanical performance of additively manufactured meta-biomaterials. Acta Biomater. 85:41–59.

Zadpoor AA. 2020. Meta-biomaterials. Biomater Sci. 8(1):18–38.

Zhang X-c, An C-c, Shen Z-f, Wu H-x, Yang W-g, Bai J-p. 2020. Dynamic crushing responses of bio-inspired reentrant auxetic honeycombs under in-plane impact loading. Mater Today Commun. 23:100918.